

# The helium isotopic ratio in the solar wind and ion fractionation in the corona by inefficient Coulomb drag

Roland Bodmer\* and Peter Bochsler

Physikalisches Institut, University of Bern, Sidlerstrasse 5, CH-3012 Bern, Switzerland

Received 8 April 1998 / Accepted 17 June 1998

**Abstract.** Using data obtained between 1991 and 1996 with the SWICS instrument (Solar Wind Ion Composition Spectrometer) aboard the Ulysses spacecraft, a long time average of the ( $^4\text{He}/^3\text{He}$ ) isotopic ratio of  $2450 \pm 460$  in coronal hole dominated solar wind is derived. To assess the influence of inefficient Coulomb friction in the inner corona and to infer the solar photospheric abundance ratio from the solar wind flux ratio, the variation of the fluxes with different solar wind regimes is investigated and limits for the long time fractionation effects are given. Finally a present-day  $^4\text{He}/^3\text{He}$  abundance ratio in the outer convective zone of  $(^4\text{He}/^3\text{He})_{\text{OCZ}} = 2670 \pm 500$  is derived.

**Key words:** Sun: abundances – Sun: corona – solar wind – interplanetary medium

## 1. Introduction

The first in-situ determination of the ( $^4\text{He}/^3\text{He}$ ) isotopic abundance ratio with the Apollo Foil Experiment (Geiss et al. 1972) yielded the surprising result that the presolar deuterium abundance differed from the terrestrial and meteoritic abundance by as much as a factor of 6 (Geiss & Reeves 1972). This was the first conclusive evidence that the terrestrial (and meteoritic) deuterium abundance did not reflect the cosmic D/H ratio and that the presolar value derived from the isotopic composition of helium in the solar wind should be used to parameterize models of the Big Bang. Since then it has been confirmed with several methods and with determinations of different in-situ instruments that the long-time average ( $^4\text{He}/^3\text{He}$ )-flux ratio in the solar wind must be somewhere within a few percent near the originally and best determined value of 2350 (Geiss et al. 1972). The present-day isotopic ratio at the solar surface inferred from solar wind determinations has also been shown to be incompatible with non-standard solar models invoking strong internal mixing or mass loss after the onset of hydrogen burning (cf. Bochsler et al. 1990).

Inference of the helium isotopic ratio in the outer convective zone from solar wind flux ratios requires understanding the

processes which have the potential of fractionating this ratio between the Sun and the interplanetary medium where in situ samples are finally taken. There are basically three approaches for such inferences:

- (i) comparison of elemental ratios observed at the solar surface and measured in the solar wind,
- (ii) observation of variations of the helium isotopic ratio in different solar wind regimes with presumably different fractionation processes, or fractionation processes with different efficiencies,
- (iii) comparison of observations with predictions of theoretical models which incorporate the relevant fractionation processes.

With respect to (i) and (iii) it is important to remember that helium as an element is depleted by typically a factor of two relative to hydrogen in the solar wind. Furthermore, strong variations of the helium abundance related to changes in the solar wind regime have been well documented (Borrini et al. 1981). The overall depletion is ascribed to the high first ionization potential of helium ("FIP-effect") (e.g. von Steiger & Geiss 1989, or Marsch et al. 1995). The strong, regime-related variations, on the other hand, have generally been attributed to insufficient Coulomb friction of protons in the inner corona (see Geiss et al. 1970, Bürgi & Geiss 1986, or Hansteen et al. 1994 for a more recent reference). As a working hypothesis for the present analysis it is assumed that models involving inefficient Coulomb drag which predict the correct overall helium depletion in the solar wind and the observed magnitude of variations of the *elemental* He/H abundance ratio deserve some credibility also to predict the correct *isotopic* fractionation factors.

To obtain a best estimate of the ( $^4\text{He}/^3\text{He}$ ) abundance ratio in the contemporaneous outer convective zone of the Sun, this work mainly uses approach (ii). Applying new data from SWICS/Ulysses, a systematic search for trends of the ( $^4\text{He}/^3\text{He}$ ) flux ratios in the solar wind with different solar wind regimes will be presented. The abundance ratio in the solar wind source region will then be inferred from the  $^4\text{He}/^3\text{He}$  ratios measured during regimes which are least suspect for generating isotopic fractionation effects. Finally, an estimate of the uncertainty of the ( $^4\text{He}/^3\text{He}$ ) abundance ratio in the present-day outer convective zone of the Sun will be given.

\* Present address: Max-Planck-Institut für Aeronomie, D-37191 Katlenburg-Lindau, Germany

## 2. Instrumental

The SWICS experiment (Solar Wind Ion Composition Spectrometer) aboard the Ulysses spacecraft is the first Time-Of-Flight Spectrometer flown in a dedicated heliospheric mission (Gloeckler et al. 1983). SWICS is the result of the collaboration of the University of Maryland, the University of Bern, the Max-Planck Institute for Aeronomy in Lindau/D and of the Technische Universität Braunschweig under the lead of the University of Maryland (G. Gloeckler, PI). Its principle of operation is based on the technique of particle identification using a combination of electrostatic deflection, post-acceleration, and a Time-Of-Flight and energy measurement. Its first basic advantage over previously flown instrumentation consists of the fact that one-dimensional energy per charge scans produce multidimensional information on individual particles (mass, charge, and energy). The multidimensionality of the information on individual particles then helps to unambiguously distinguish between different species, even in the case of abundance ratios of several orders of magnitude, and furthermore, to discriminate particle counts from accidental background counts which are always encountered with the application of sensitive detectors in space instrumentation.

An important asset of this instrument is that due to the post-acceleration step following the energy/charge identification, the sensitivity of the sensor depends only weakly on particle energy and mass. In the case of helium, however, with its low ionic charge of 2, the post-acceleration voltage of 23 kV is near the threshold to produce signals in the solid-state energy detector. Consequently, the derivation of unbiased ( $^4\text{He}/^3\text{He}$ ) flux ratios crucially depends on a careful calibration of the energy detector for both species. With the calibration of the instrument and with further tests involving the two helium isotopes, it has been demonstrated (Bodmer 1996) that the solid-state detector efficiency of SWICS depends essentially on the particle energy and not on the mass of the particle.

## 3. Data selection and data reduction

Fig. 1 is an overview of the selected period which lasted almost six years and which began one year before the Jupiter encounter of Ulysses. The lowermost panel shows the solar wind proton velocity. He/H abundance ratio,  $^4\text{He}$  flux, the  $^3\text{He}$  flux and the ( $^4\text{He}/^3\text{He}$ ) flux ratio are shown in the other panels. The period begins with approximately 500 days of in-ecliptic solar wind, followed by a period of approximately 400 days when Ulysses was moving across the heliographic mid-latitudes and encountered recurrent high speed streams with intermittent low speed solar wind with a very regular periodicity given by the solar rotation period. The rest of the period is characterized by the perihelion of Ulysses' orbit with a relatively fast scan from the southern polar hole over the equator to the northern polar hole. The selected period covers about the entire decline of solar cycle 22 and it includes a significant fraction of coronal-hole associated solar wind. These somewhat special conditions have to be taken into account for comparison of the results of this study with long time averages from data of in-ecliptic spacecraft.

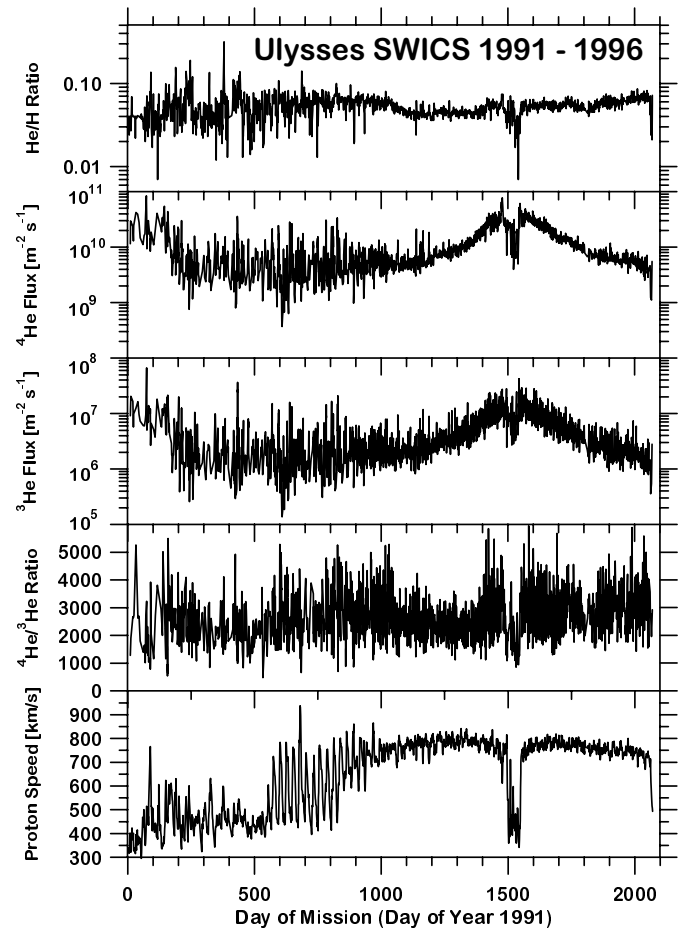


**Fig. 1.** Overview of solar wind properties during the primary Ulysses mission. Note that fluxes have not been renormalized to 1 AU distance from the Sun.

The following discussion concentrates on  $^3\text{He}$  data collected with the triple coincidence method. Some explanations of the experimental procedure are appropriate at this place. In order to be registered in the triple coincidence mode, a particle has to pass the electrostatic energy analyzer (EA), it then has to trigger a start pulse in the carbon foil of the Time-Of-Flight sensor, furthermore it must produce a stop pulse at the end of the Time-Of-Flight path, and it has to generate an energy signal in the solid state detector (SSD). The most critical issue for the reliable analysis of the helium isotopic ratio concerns the detection in the SSD. With typical solar wind velocities and a post acceleration voltage of 22.6 keV which was applied throughout the period under consideration, the energy of helium ions is often marginally above the threshold of detection. Fortunately, using a different sensor it has been possible to verify in an extensive calibration effort that both helium isotopes exhibit very similar detection efficiencies in a wide range of energies. In the solar wind the light helium isotope travels typically at the same speed as the heavy isotope, hence, its energy amounts to 3/4 of the energy of the heavy isotope. However, after post-acceleration the difference in energy and the corresponding detection efficiencies in the SSD differ only by a small amount. Thus no

strong hidden discrimination effect has to be expected, despite the strong variations in sensitivity for triple coincidence events near threshold of the SSD. The isotopic mass dependence of the other efficiencies (start detection, stop detection) and of the energy passband through the EA is less pronounced and well understood (see Bodmer (1996) for more details).

For the further analysis we have finally chosen a method in which ten consecutive  $^3\text{He}$  triple coincidence counts are put into one time bin. These bins are consequently of variable length in time; the average length of a bin is about one day. The clear advantage of such a technique is that it fixes the relative statistical uncertainty which is the most important contribution to the overall uncertainty at  $\pm 30\%$ .  $^4\text{He}$  fluxes, H fluxes, and other properties of the solar wind have then been averaged at these time bins for the detailed analysis.

#### 4. Results

Fig. 2 is a scatterplot correlating the decimal logarithms of the  $^3\text{He}$  and the  $^4\text{He}$  fluxes. The  $^3\text{He}$  fluxes are evidently well correlated with the  $^4\text{He}$  fluxes, the correlation coefficient is  $0.914 \pm 0.007$ . For the comparison with correlations determined with instruments from other spacecraft it must, however, be noted that due to the rather large spread in fluxes, observed in a wide range of radial distances from the Sun, the correlation coefficient is artificially enhanced, i.e. because the statistical variability of the  $^3\text{He}$  fluxes is favorably small compared to the extraordinarily large variability of the  $^4\text{He}$  flux which has been observed over a wide range of solar distances. If the correlation coefficient is only determined after normalizing the fluxes to 1 AU, the variability of the fluxes is correspondingly reduced to temporal variations only, and the correlation coefficient decreases to  $0.820 \pm 0.013$ . The full straight line in Fig. 2 indicates a fixed abundance ratio of  $^4\text{He}/^3\text{He} = 2500$ , the dashed lines show constant ratios of 2000 and 3000, respectively.

To obtain the best estimate of the flux ratio in the solar wind and for comparison with other observations it is best to take the ratio of the integrated fluxes of the two isotopes, or, equivalently, the ratio of the temporal averages of fluxes. The given uncertainty of this ratio rests largely on the uncertainty of the relative sensitivities of the instrument for the two isotopes. We estimate this uncertainty to be 20%, and we conclude that the overall flux ratio for the period from 1991 through 1996 derived from Ulysses/SWICS data is

$$^4\text{He}/^3\text{He} = 2450 \pm 460.$$

Fig. 3 shows the distribution of the single determinations obtained with the above method using bins with ten triple coincidences of  $^3\text{He}$ . The fluxes have been normalized to 1 AU. Despite the good correlation of the fluxes of the two helium isotopes, resulting in a rather narrow distribution of the abundance ratios, it is evident that the distribution of the  $^3\text{He}$  fluxes is wider than the distribution of the  $^4\text{He}$  fluxes. Since the relative statistical uncertainty of the  $^3\text{He}$  abundance measurements amounts to 30%, the contribution of statistics to the width of

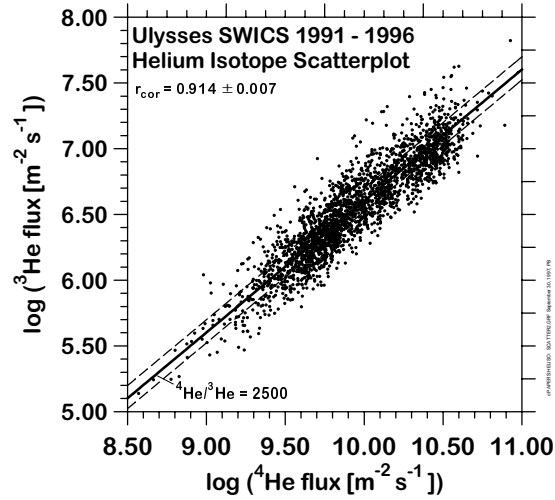


Fig. 2. Scatter plot of fluxes of the two helium isotopes. The full line connects points with  $^4\text{He}/^3\text{He}$  abundance ratios of 2500. The upper and lower dashed lines connect points with ratios of 2000 and 3000 respectively. The fluxes have not been normalized to 1 AU.

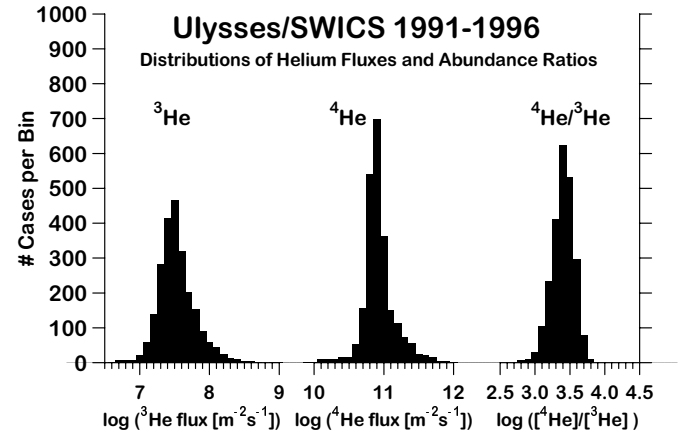
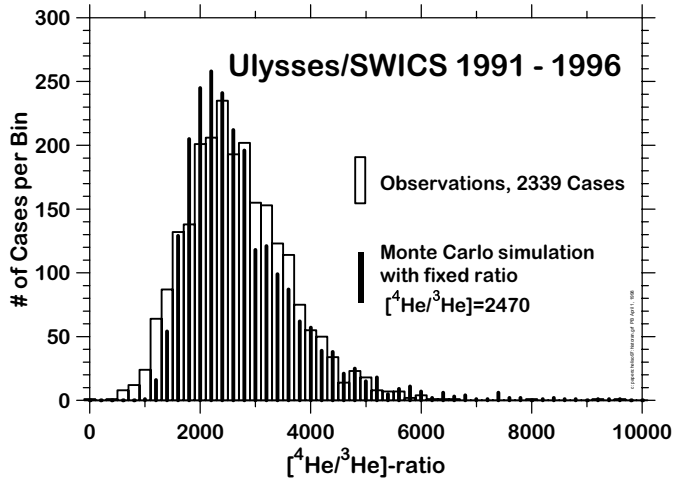


Fig. 3. Histograms of logarithms of fluxes of the helium isotopes and logarithms of the isotopic abundance ratio derived from five years including 2339 observations. The width of the  $^4\text{He}$  flux distribution reflects essentially the natural fluctuations of  $^4\text{He}$  in the solar wind. The width of the observed  $^3\text{He}$  distribution is partially caused by natural fluctuations and partially due to the statistical uncertainties of the 10-count method.

the  $\log(^3\text{He flux})$  distribution is 0.13. The observed standard deviation of the distribution is 0.27, roughly twice the amount expected from statistical uncertainties.

In view of the low count rates and of the related large statistical uncertainties of the observed  $^3\text{He}$  fluxes, we have to address the question as to how much of the observed fluctuations of the helium isotope ratio are real and how much is caused by counting statistics. The deviations from the full line in Fig. 2 which indicates a fixed ratio, are sometimes quite substantial. On the other hand it is clear that even with a fixed count number of  $^3\text{He}$  events, as used for the determination of the abundance ratio, occasional excursions might occur. Fig. 4 compares the observed abundance ratios on a linear scale with the result of a



**Fig. 4.** Comparison of observed  $^4\text{He}/^3\text{He}$  abundance ratios with results from a Monte Carlo simulation of  $^3\text{He}$  counts and  $^4\text{He}$  counts, assuming a fixed isotopic ratio of 2670. The abundance ratios are calculated after the accumulation of ten  $^3\text{He}$  counts (and usually many more  $^4\text{He}$  counts). The appearance of the histogram of observations suggests that at least part of the variations are real, i.e. cases with  $^4\text{He}/^3\text{He} \approx 1000$  - 1500, as well as cases with  $^4\text{He}/^3\text{He} \approx 3000$  are overrepresented if compared to the simulation with a fixed ratio.

Monte Carlo simulation in which  $^4\text{He}$  counts and  $^3\text{He}$  counts occur independently and randomly distributed over time but the  $^4\text{He}$  rate is set so that the  $^4\text{He}/^3\text{He}$  ratio is constant on average. After ten  $^3\text{He}$  events have been counted the  $^4\text{He}$  summation is stopped as well and the result is registered in the histogram in Fig. 4 with full bars. At first sight a rather close similarity between the observed (empty bars) and the simulated distribution is evident. Closer inspection shows that the observations are, however, somewhat more widely spread in the range of ratios from 1000 to 3000 than expected from the statistical simulation, suggesting that a fixed solar wind  $^4\text{He}/^3\text{He}$  abundance ratio and counting statistics cannot account for the observations, and that some of the observed variability is due to real variations of the isotopic helium abundance ratio in the solar wind.

## 5. Discussion

The most likely cause for fluctuations of the  $^4\text{He}/^3\text{He}$  ratio in the solar wind is inefficient Coulomb drag. The most sensitive indicator for this effect is variability of the elemental He/H abundance ratio. Whereas wave pressure (and/or efficient Coulomb friction with protons) seem to efficiently accelerate helium and minor species in the coronal hole associated fast speed streams, helium is sometimes strongly depleted in low-speed solar wind flowing near the interplanetary current sheet (Borriani et al. 1980). Even if the scenario envisioned here which places the most important elemental and isotopic effects in the inner corona is incorrect or only partially correct, the conclusion about sign and the expected order of magnitude of the effect should nevertheless be valid: If collisions in the chromosphere fractionate the He/H elemental ratio (as proposed by Hansteen et al. (1997)), or in the inner corona (as discussed e.g. by Bürgi

& Geiss (1986) or by Bodmer & Bochsler (1998)) the concomitant predicted amount of isotopic fractionation of the  $^4\text{He}/^3\text{He}$  ratio should roughly be correct. From theoretical models explaining the elemental fractionation ascribed to the so-called FIP effect, it is generally concluded that isotopic fractionation effects, even those involving  $^3\text{He}$  and  $^4\text{He}$  with a relative mass difference of 25%, are minute (v. Steiger & Geiss, 1989; Marsch et al. 1995; Peter 1996). For instance, Marsch et al. (1995) have given a simple expression for the asymptotic dependence of the FIP fractionation of two species  $j, k$

$$f_{jk} \approx \frac{r_{kH}}{r_{jH}} \sqrt{\frac{\tau_k}{\tau_j}} \left( \frac{A_j + 1}{A_j} \frac{A_k}{A_k + 1} \right)^{1/4}, \quad (1)$$

where  $f_{jk}$  is the estimated enrichment factor of  $(n_j/n_k)$ ,  $r_{iH}$  the collisional radius of species  $i$  with neutral hydrogen,  $\tau_i$  is the first ionization time, and  $A_i$  is the atomic mass of species  $i$ . In the process described by Marsch et al. (1995), the atomic mass only plays a rôle in the mobility of the species in a collision-dominated gas and, hence, it only appears in the fourth root of the mass ratio, slightly favoring the lighter species. For the case of the two helium isotopes, a factor  $f_{34} \approx 1.016$  is obtained from the above expression. Even if other processes than the FIP mechanism could play an important rôle in the chromosphere (e.g. Hansteen et al. 1997), the quoted models succeed to qualitatively and quantitatively reproduce the elemental abundance pattern in the solar wind. Hence, the conclusion that the chromospheric FIP process is unable to produce a substantial helium isotopic fractionation in the solar wind seems no too far fetched.

In the sense of the arguments outlined above, it seems useful to investigate the correlation between the  $^3\text{He}/\text{H}$  abundance ratio with the He/H ratio in different types of solar wind regimes. Solar wind regimes producing relatively high He/H abundance ratios are also expected to produce elevated  $^3\text{He}/\text{H}$  ratios. Such a trend is indeed observed in the scatter plot shown in Fig. 5. However, it must be emphasized that such a trend would even appear in the case of completely independent random variables with fluctuations of similar variance. In fact, denoting the logarithms of the hydrogen flux with  $f_H$ , and the logarithms of the fluxes of the two helium isotopes, correspondingly, with  $f_3$  and  $f_4$ , the logarithms of the He/H- and the  $^3\text{He}/\text{H}$  ratio with  $r_{41}$  and  $r_{31}$ , the following relation is found for the correlation coefficient between  $r_{41}$  and  $r_{31}$ :

$$r_{cor}(r_{41}, r_{31}) = \frac{\text{var}(f_H)}{\sqrt{\text{var}(r_{41})\text{var}(r_{31})}} \frac{r_{cor}(f_H, f_4) \sqrt{\text{var}(f_H)\text{var}(f_4)}}{\sqrt{\text{var}(r_{41})\text{var}(r_{31})}} - \frac{r_{cor}(f_H, f_3) \sqrt{\text{var}(f_H)\text{var}(f_3)}}{\sqrt{\text{var}(r_{41})\text{var}(r_{31})}} + \frac{r_{cor}(f_3, f_4) \sqrt{\text{var}(f_3)\text{var}(f_4)}}{\sqrt{\text{var}(r_{41})\text{var}(r_{31})}} \quad (2)$$

Here,  $\text{var}(f)$  is the variance of the random variable  $f$ . For the case of equal variances of the fluxes of all three species considered this relation reduces to

$$r_{cor}(r_{41}, r_{31}) = \quad (3)$$

$$\frac{1 - r_{cor}(f_H, f_4) - r_{cor}(f_H, f_3) + r_{cor}(f_3, f_4)}{2\sqrt{(1 - r_{cor}(f_H, f_4))(1 - r_{cor}(f_3, f_H))}}$$

It is immediately evident that in the case of fully uncorrelated variabilities of  $f_H$ ,  $f_4$ , and  $f_3$ , a correlation coefficient of the ratios of 0.5 is obtained, merely a consequence of the use of a common denominator. The measured correlation coefficient is  $0.517 \pm 0.030$ , not far from the value expected for a completely uncorrelated variability of the fluxes. Hence, judging from the correlation of the isotopic ratio with the He/H elemental ratio, no evidence for a rôle of inefficient Coulomb drag is obvious. This negative result has either to be ascribed to statistical uncertainties in the observations or to other processes which could, for instance, affect the He/H ratio in a manner which is not included in this consideration, thereby masking a possible correlation.

Bodmer & Bochsler (1998) who investigate the rôle of Coulomb drag in fractionating isotopic abundances use the following asymptotic expression to describe the motion of minor species under the influence of strong Coulomb friction by protons

$$u_{xo} = u_{po} \left( 1 - \frac{2A_x - Q_x - 1}{Q_x^2} \sqrt{\frac{A_x + 1}{A_x}} \frac{C_p}{n_{po} u_{po}} \right), \quad (4)$$

where  $u_x$  and  $u_p$  are the asymptotic speeds at the coronal base of the test- and field particles, respectively.  $A_x$  and  $Q_x$  are atomic mass and charge number of the test particles,  $C_p$  is a species-independent parameter describing the gravitational force in relation to the Coulomb drag force, and  $n_p$  is the density of field particles (protons). From the condition of conservation of particle fluxes  $\Phi_x$  which is valid along a given flux tube one obtains the relation

$$\frac{\Phi_x}{\Phi_p} = \frac{n_x u_x}{n_p u_p} = \frac{n_{xo} u_{xo}}{n_{po} u_{po}}. \quad (5)$$

Defining the fractionation factor  $f_x = \Phi_x/n_{xo}$  as the flux  $\Phi_x$  of species  $x$  in the solar wind relative to its density  $n_{xo}$  at the coronal base one obtains from expression (5)

$$\frac{f_x}{f_p} = \frac{u_{xo}}{u_{po}} = 1 - F_x \frac{C_p}{n_{po} u_{po}}, \quad (6)$$

with

$$F_x = \frac{2A_x - Q_x - 1}{Q_x^2} \sqrt{\frac{A_x + 1}{A_x}}. \quad (7)$$

The factors  $C_p/n_{po}u_{po}$  can be eliminated if fractionation factors of two minor species are compared according to relation

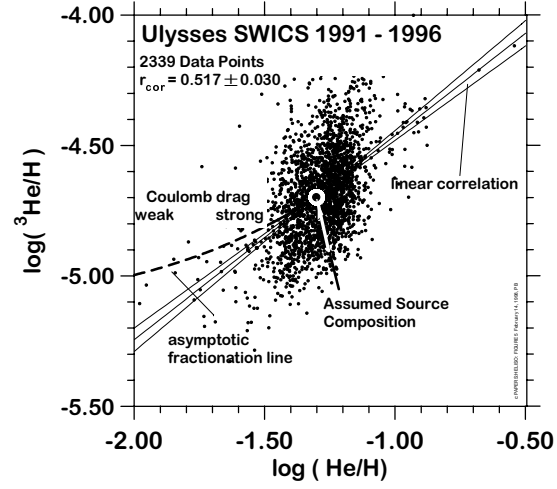


**Fig. 5.** Helium isotope scatter plot showing the relation between observed  ${}^3\text{He}/\text{H}$  and  ${}^4\text{He}/\text{H}$  abundance ratios. The linear correlation scissors are illustrated with thin lines, the thick dashed line shows an approximate path of variability as expected from the effect of varying Coulomb drag, originating from a source composition indicated by the black dot

(6). For instance, the fractionation factor  $f_3$  for  ${}^3\text{He}$  can now be put into relation to  $f_4$ , i.e.

$$\frac{f_3}{f_p} = 1 - \frac{F_3}{f_4} \left( 1 - \frac{f_4}{f_p} \right). \quad (8)$$

Finally, the following relation is obtained in a straightforward manner

$$\log \left( \frac{[{}^3\text{He}]}{[\text{H}]} \right)_{\text{sw}} = \log \left( \frac{[{}^3\text{He}]}{[\text{H}]} \right)_{\text{source}} + \log \left( 1 - \frac{F_3}{F_4} \left( 1 - \frac{[\text{He}]/[\text{H}]_{\text{sw}}}{[\text{He}]/[\text{H}]_{\text{source}}} \right) \right), \quad (9)$$

with  $F_3/F_4 = 0.62$ .

Relation (9) is delineated in Fig. 5 with a fat line. It approximates the situation in a regime with efficient Coulomb drag, i.e. when the fractionation factors are close to 1, and it is less reliable for regimes with inefficient Coulomb drag. In this range the curve is continued as a dashed line. The source composition which is used to fix the curve is indicated with a white circle. Again, no trend suggesting any importance of this effect is evident from the observations shown in Fig. 5, and again, the conclusion must be that the discussed effect is either absent, masked by statistical uncertainties of the observations, or overruled by other - more important - processes in the solar wind.

Fig. 6 outlines the distribution of logarithms of the  ${}^4\text{He}/{}^3\text{He}$  abundance ratios versus solar wind speed. The most conspicuous feature is a bimodal distribution of cases showing that the data set is strongly biased towards high speed solar wind ( $v \sim 800$  km/s). The sequence of the contour lines of the two

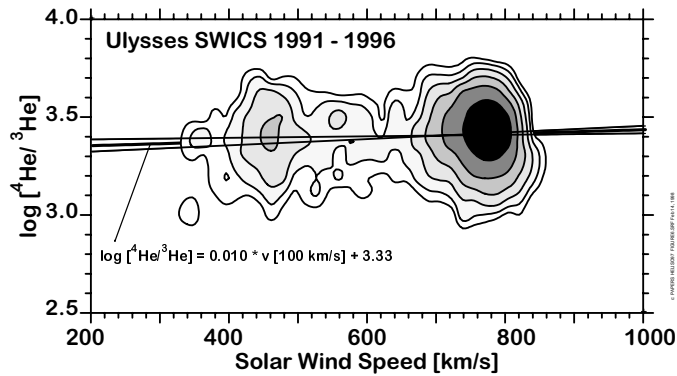


**Fig. 6.**  $\log^4\text{He}/^3\text{He}$  vs solar wind speed. Contour lines delineate 2,4,8,16,32, and 64 cases per bin. The full lines show the correlation scissors. A weak increase from  $3.37(^4\text{He}/^3\text{He} = 2350)$  to  $3.41(^4\text{He}/^3\text{He} = 2570)$  is indicated in the velocity interval from 400 to 800 km/s.

prominent maxima indicates that in general, the variability of the isotope ratio is larger in the low speed wind than in the high speed wind, i.e. despite the fact that many more cases are in the high speed maximum, its dispersion is not larger than the width of the low speed maximum. A similar observation with SWICS/Ulysses has recently been reported by Gloeckler and Geiss (1998).

Comparing then the  $^4\text{He}/^3\text{He}$  ratios for the two flow regimes a weak trend is found, indicating that the isotope ratio increases from typically 2350 for the low speed solar wind to typically 2570 for the high speed wind.

Now, the trend of increasing  $^4\text{He}/^3\text{He}$  ratios with increasing solar wind speed seems marginally significant. The sign and order of magnitude correspond to the expectations about the efficiency of Coulomb drag at low solar wind speeds.

Finally, we make an attempt to estimate the unfractionated  $^4\text{He}/^3\text{He}$  abundance ratio from the observations and the discussion as outlined above. As a lower limit we assume the high speed ratio, i.e. we assume

$$(^4\text{He}/^3\text{He})_{OCZ} > 2570 \quad (10)$$

For the other extreme, we assume that even the observed high speed ratio is still fractionated by a factor 0.93 compared to the source composition. From this we conclude that

$$(^4\text{He}/^3\text{He})_{OCZ} < 2760. \quad (11)$$

To obtain a final estimate, the experimental uncertainties of the observations must also be taken into account. Since they are independent from the model extrapolation we add them squarely to the model uncertainties and obtain

$$(^4\text{He}/^3\text{He})_{OCZ} = 2670 \pm 500. \quad (12)$$

## 6. Conclusions

The  $^4\text{He}/^3\text{He}$  abundance ratio is the one which is most susceptible to processes which can selectively affect species according to their masses. From the observations of Ulysses

/SWICS carried out over six years and covering a large fraction of high speed solar wind, a rather weak trend over different flow regimes is found. This leads to the conclusion that the solar wind, in particular the high speed solar wind, reflects solar surface isotopic abundances rather well. According to our experimental and theoretical considerations, a relative difference of  $\sim 7\%$  from the source has to be expected between the  $^4\text{He}/^3\text{He}$  ratio in coronal hole associated solar wind and the source, and a difference of the order of 16% for interstream solar wind. This confirms earlier estimates of Geiss & Bochsler (1991).

The result also limits the range of possible fractionation effects to be expected for other isotopic abundance ratios which are now at the fringes of being detectable (Bochsler et al. 1995, Kallenbach et al. 1997, Kucharek et al. 1998). Hence, derivation of solar isotopic abundance ratios from solar wind values seems definitely feasible within uncertainties of 1% or less. This is of major importance for the interpretation of results of ongoing (SOHO, WIND, ACE) and upcoming missions (GENESIS).

*Acknowledgements.* We gratefully acknowledge helpful discussions with G.Gloeckler, J. Geiss and R. von Steiger. R. Wimmer, R. Neukomm and M.R. Aellig have been helpful in clarifying several instrumental aspects. We also appreciate valuable comments by the referee, V.H. Hansteen. B. Grose converted the manuscript into its camera-ready form. This work was supported by the Swiss National Science Foundation.

## References

- Bochsler P., Geiss J., and Maeder A.: 1990, The abundance of  $^3\text{He}$  in the solar wind - a constraint for models of solar evolution. *Solar Physics* 128, 203-215
- Bochsler P., Gonin M., Sheldon R.B. et al.: 1996, Abundance of solar wind magnesium isotopes determined with WIND/MASS. In: *Solar Wind Eight. Proceedings of the Eighth International Solar Wind Conference*, Winterhalter, D., Gosling J.T., Habbal S.R., Kurth W.S., and Neugebauer M. (eds.) AIP Conference Proceedings 382. Woodbury, N.Y., 199-202
- Bodmer R.: 1996, The helium isotopic ratio as a test for minor ion fractionation in the solar wind acceleration process: SWICS/ULYSSES data compared with results from a multifluid model. Thesis. University of Bern
- Borriani G., Gosling J.T., Bame S.J., Feldman W.C., and Wilcox J.M.: 1981, Solar wind helium and hydrogen structure near the heliospheric current sheet: A signal of coronal streamers at 1AU, *J. Geophys. Res.* 86, 4565-4573
- Bürgi A. and Geiss J.: 1986, Helium and minor ions in the corona and solar wind: Dynamics and charge states *Solar Physics* 103, 347-383
- Geiss J. and Bochsler P.: 1991, Long time variations in solar wind properties: Possible causes versus observations. In: *The Sun in Time*, Sonett C.P., Giampapa M.S., and Matthews M.S. (eds.) pp. 98-117. Univ. Arizona Press, Tucson, Arizona
- Geiss J., Bühler F., Cerutti H., Eberhardt P., and Filleux C.: 1972, Solar wind composition experiment Apollo 16, Prelim. Sci. Rep. NASA SP-315, 14.1-14.10
- Geiss J., Hirt P., and Leutwyler H.: 1970, On acceleration and motion of ions in corona and solar wind, *Solar Physics* 12, 458-483.
- Geiss J., and Reeves H.: 1972, Cosmic and solar system abundances of deuterium and helium-3, *Astron. Astrophys.* 18, 126-132.

- Gloeckler G., and Geiss J.: 1998, Measurement of the abundance of Helium-3 in the Sun and in the local interstellar cloud with SWICS on Ulysses. In: Proceedings of the ISSI workshop on the local interstellar medium, Bern 1997, in press
- Gloeckler G., Geiss J., Balsiger H. et al.: 1983, The ISPM solar-wind ion composition spectrometer, ESA SP-1050, 75-103
- Hansteen V.H., Leer E., and Holzer T.E.: 1994, Coupling of the coronal helium abundance to the solar wind, *Astrophys. J.* 428, 843-853
- Hansteen V.H., Leer E., and Holzer T.E.: 1997, The role of helium in the outer solar atmosphere. *Astrophys. J.* 482, 498-509
- Kallenbach R., Ipavich F.M., Bochsler P. et al.: 1997, Isotopic composition of solar wind neon measured by CELIAS/MTOF on board SOHO, *J. Geophys. Res.* 102, 26895-26904
- Kucharek H., Ipavich F.M., Kallenbach R. et al., 1998, Magnesium isotopic composition as observed with the MTOF sensor of the CELIAS experiment on the SOHO spacecraft, submitted to *J. Geophys. Res.*
- Marsch E., von Steiger R. and Bochsler P.: 1995, Element fractionation by diffusion in the solar chromosphere. *Astron. Astrophys.* 301, 261-276
- Peter H.: 1996, Velocity-dependent fractionation in the solar chromosphere. *Astron. Astrophys.* 312, L37-L40.
- Von Steiger R., and Geiss J.: 1989, Supply of fractionated gases to the corona. *Astron. Astrophys.* 225, 222-238